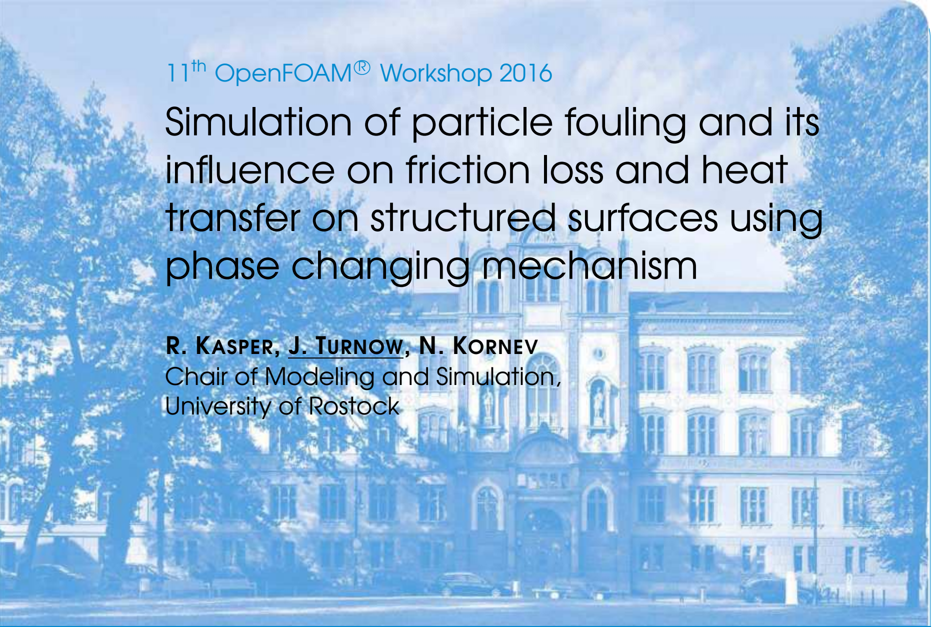

11th OpenFOAM® Workshop 2016

Simulation of particle fouling and its influence on friction loss and heat transfer on structured surfaces using phase changing mechanism

R. Kasper, J. Turnow, N. Kornev
Chair of Modeling and Simulation,
University of Rostock

Outline

Introduction

Modeling and implementation
- Euler-Lagrange approach
- Lagrangian particle tracking
- Deposition of particles
- Reaction of the particulate fouling on the carrier fluid
- Heat transfer
- Erosion of the fouling layer

Results
- Validation and verification of the Lagrangian particle tracking
- Particulate fouling on structured heat transfer surfaces

Conclusion and outlook

Outline

Motivation

- Heat transfer enhancement using structured heat transfer surfaces
- Assessment of heat transfer enhancement through thermohydraulic efficiency
  $\Rightarrow$ Best performance: **V**ortex **H**eat **T**ransfer **E**nhancement (VHTE)
- **Problem:** structured surfaces causes particulate fouling, i.e. undesirable deposition of suspended solid particles (e.g. sand, rust or dirt)

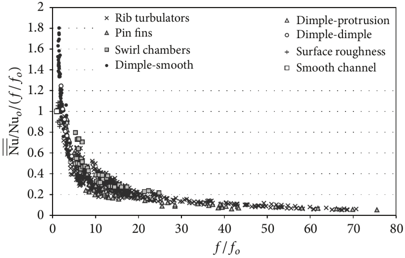

Figure: Thermohydraulic efficiency [Ligrani et al., 2013]

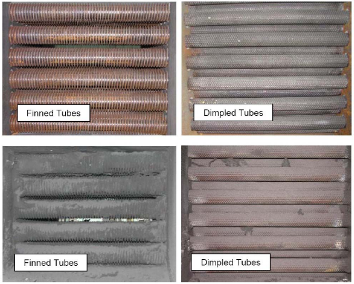

Figure: Particulate foulingin heat exchangern [Chudnovsky et al., 2008]

Motivation

- Evaluation of the thermohydraulic efficiency with respect to particulate fouling
- Insufficient knowledge about the interaction between particulate fouling and local vortex structures
- Available fouling models are mostly too specific and depending on an abundance of empirical constants

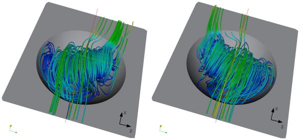

Figure: Dimple flow (Turnow et al., 2012)

⇒ **Development of an universal method for the determination and analysis of particulate fouling and its interaction with local vortex structures**

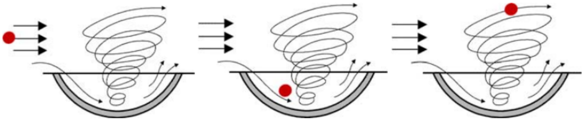

Figure: Mechanism of the fouling mitigation potential of a single dimple (Chudnovsky et al., 2008)

Outline

Lagrangian particle tracking

- Continuous phase (carrier fluid):

$$\nabla \cdot \boldsymbol{u} = 0 \tag{1}$$

$$\rho \left(\frac{\partial \boldsymbol{u}}{\partial t} + (\boldsymbol{u} \cdot \nabla \boldsymbol{u}) \right) = -\nabla p + \mu \nabla^2 \boldsymbol{u} - \boldsymbol{S} \tag{2}$$

- Dispersed phase (solid particles):

$$\frac{\mathrm{d}\boldsymbol{x}_p}{\mathrm{d}t} = \boldsymbol{u}_p \tag{3}$$

$$m_p \frac{\mathrm{d}\boldsymbol{u}_p}{\mathrm{d}t} = \sum \boldsymbol{F}_i \tag{4}$$

$$I_p \frac{\mathrm{d}\boldsymbol{\omega}_p}{\mathrm{d}t} = \sum \boldsymbol{T} \tag{5}$$

- Computation of the particle trajectories using Lagrangian particle tracking (LPT) → the most natural way in order to describe the physics of suspended solid particles
- Present Euler-Lagrange approach is capable to take one-, two- and four-way coupling into account

Lagrangian particle tracking

- In order to calculate the trajectories of the suspended particles, the sum of all acting forces is needed:

$$m_p \frac{\mathrm{d}\boldsymbol{u}_p}{\mathrm{d}t} = \sum \boldsymbol{F}_i = \boldsymbol{F_D} + \boldsymbol{F_G} + \boldsymbol{F_P} + \boldsymbol{F_A} \tag{6}$$

  - Drag force:

$$\boldsymbol{F_D} = m \frac{\mathrm{d}\boldsymbol{u_p}}{\mathrm{d}t} = \frac{1}{2} C_D \frac{\pi D^2}{4} \rho_c \left(\boldsymbol{u} - \boldsymbol{u_p}\right) \left|\boldsymbol{u} - \boldsymbol{u_p}\right| \tag{7}$$

$$C_D \mathrm{Re}_p = \begin{cases} 24\left(1 + \frac{1}{6}\mathrm{Re}_p^{2/3}\right) & \text{if } \mathrm{Re}_p \leq 1000 \\ 0.424 \mathrm{Re}_p & \text{if } \mathrm{Re}_p > 1000 \end{cases} \tag{8}$$

  - Gravitational and buoyancy force:

$$\boldsymbol{F_G} = m_p \boldsymbol{g} \left(1 - \frac{\rho_c}{\rho_p}\right) \tag{9}$$

  - Pressure gradient and added mass force:

$$\boldsymbol{F_P} = \rho_c \frac{\pi D^3}{6} \left(\frac{\mathrm{D}\boldsymbol{u}}{\mathrm{D}t} - \nu \nabla^2 \boldsymbol{u}\right), \quad \boldsymbol{F_A} = C_A \rho_c \frac{\pi D^3}{6} \left(\frac{\mathrm{D}\boldsymbol{u}}{\mathrm{D}t} - \frac{\mathrm{D}\boldsymbol{u_p}}{\mathrm{D}t}\right) \tag{10}$$

Deposition of particles

- Condition for particle deposition:

$$\boldsymbol{u}_p / \boldsymbol{u}_\infty = 0.0001, \;\; \Delta t \geq 0.5\,\text{s} \tag{11}$$

- Introduction of an additional continuous phase for deposited particles (fouling layer):

$$\alpha_{new,i} = \alpha_{old,i} + \frac{V_{particle}}{V_{cell}} \tag{12}$$

- Distribution of the fouling phase depends on the local cell based phase gradient $\nabla\alpha$

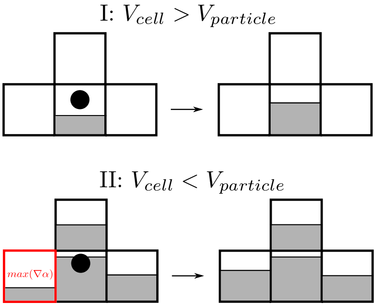

Figure: Conversion algorithm

- Linear interpolation of the physical properties x_i (i.e. viscosity, density or thermal conductivity) with respect to the phase fraction:

$$x_i = \alpha \cdot x_{fouling} + (1 - \alpha) \cdot x_{fluid} \tag{13}$$

Reaction of the particulate fouling on the carrier fluid

- Fouling phase as porous medium with isotropic permeability
- Local flow resistance due to particulate fouling as additional source term of the momentum balance (Darcy's law):

$$\boldsymbol{S} = \alpha \frac{\mu}{K} \boldsymbol{u} \qquad (14)$$

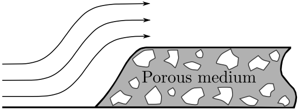

Figure: Porous medium

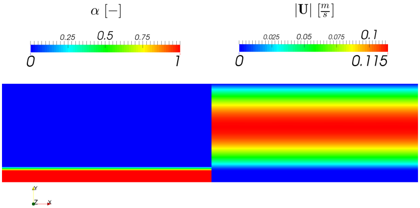

Figure: Influence of the permeability of a constant fouling layer on the velocity profile for a laminar channel flow ($h_f = 0.002\,\mathrm{mm}$)

Heat transfer

- Simulation of heat transfer due to convection and diffusion by use of simplified energy conservation equation → actual no consideration of thermophoresis effects:

$$\frac{\partial T}{\partial t} + \nabla \cdot (\boldsymbol{u} T) = \nabla^2 \left(a_{eff}(\alpha) T\right) \quad \text{with} \quad a_{eff}(\alpha) = \frac{\nu(\alpha)}{\mathrm{Pr}(\alpha)} + \frac{\nu_t}{\mathrm{Pr}_t(\alpha)} \tag{15}$$

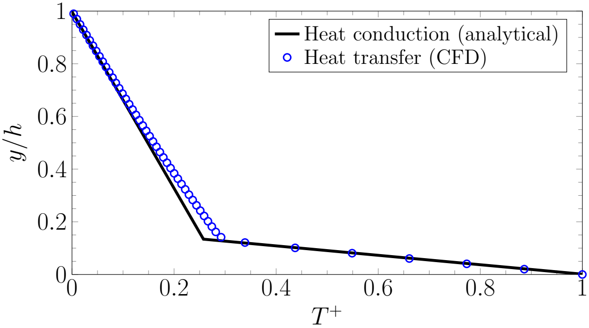

Figure: Temperature profile / fouling resistance for a laminar channel flow with a constant fouling layer ($h_f = 0.002\,\mathrm{mm}$)

Erosion of the fouling layer

- Return of deposited particles into the LPT possible
- Computation of the degraded fouling phase and the number of particles:

$$\alpha_{removed} = \frac{V_{particle}}{\tau_{rel}} \cdot \frac{|\tau_{cell}|}{V_{cell}}, \quad n = \left(\frac{6 \cdot \alpha_{removed} \cdot V_{particle}}{\pi}\right)^{1/3} \cdot \frac{1}{d_{particle}} \tag{16}$$

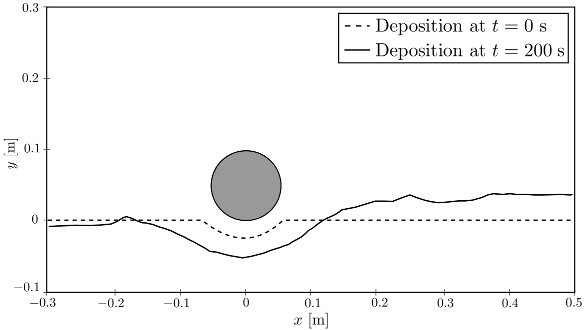

Figure: Flow around a cylinder over a predefined bed of particulate fouling

Outline

Validation and verification of the Lagrangian particle tracking using Taylor-Green vortex

Validation and verification of LPT through the analytical solution of the Taylor-Green vortex (2D):

- Streamfunction:

$$\Psi(x,\ y,\ t) = \frac{\omega_0}{k^2}\cos(k_x x)\cos(k_y y)\exp(-\mathrm{Re}_0^{-1} k^2 t) \tag{17}$$

- Components of the fluid velocity:

$$u_x = \frac{\partial \Psi}{\partial y} = -\omega_0 \frac{k_y}{k^2}\cos(k_x x)\sin(k_y y)\exp(-\mathrm{Re}_0^{-1} k^2 t) \tag{18}$$

$$u_y = -\frac{\partial \Psi}{\partial x} = \omega_0 \frac{k_x}{k^2}\sin(k_x x)\cos(k_y y)\exp(-\mathrm{Re}_0^{-1} k^2 t) \tag{19}$$

- Chosen parameters: $k^2 = k_x^2 + k_y^2$, $k_x = k_y = 1$, $\omega_0 = 2$, $\mathrm{Re}_0 = 0.004$, $0 \leq x,y \leq 2\pi$
- Assumption: no gravitational force

Validation and verification of the Lagrangian particle tracking using Taylor-Green vortex

- Investigation of the influence of τ_p (relaxation time of the particle) within the Stokes regime:

$$\tau_p = \frac{\rho_p D_p^2}{18\mu_f} \tag{20}$$

- For $\tau_p = 0$, particle trajectories corresponds to the streamlines

- For $\tau_p >> 0$, particle trajectories do not corresponds to the streamlines (inertia of the particles becomes more dominant)

$$\mathbf{\Psi}(x,\, y,\, t = 3.4\text{ s}),\ \tau_p = \frac{\rho_p D_p^2}{18\mu_f} \approx 0$$

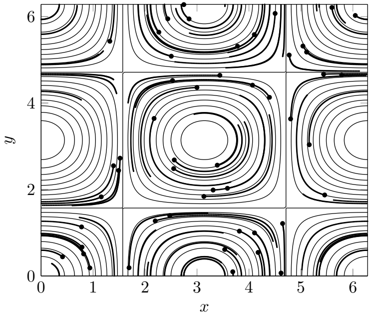

Figure: Particle trajectories for $\tau_p \approx 0$

Validation and verification of the Lagrangian particle tracking using Taylor-Green vortex

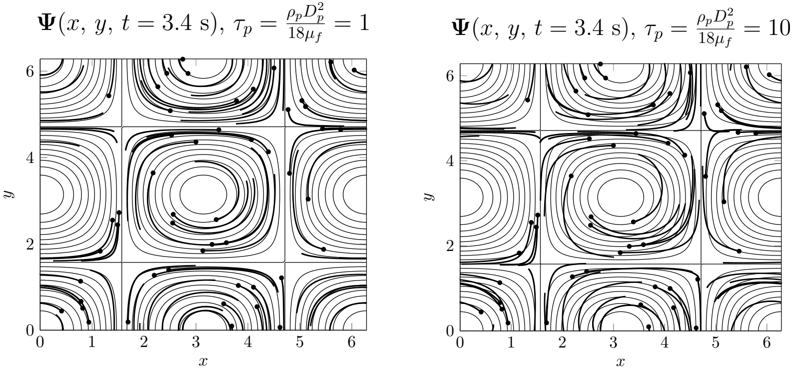

Figure: Particle trajectories for $\tau_p = 1$ (left) and $\tau_p = 10$ (right)

Particulate fouling on structured heat transfer surfaces

- Parameters:
  - $L/H = 18.4$, $B/H = 5.33$
  - $H/D = 0.326$, $H/T = 1.250$
  - $\mathrm{Re}_H = 1000,\ 5650$
  - $\mathrm{Pr} = 0.71$
- Large eddy simulation
- LES models: DSM, DOE
- Grid resolution: ca. 1 300 000 CV

Cavity

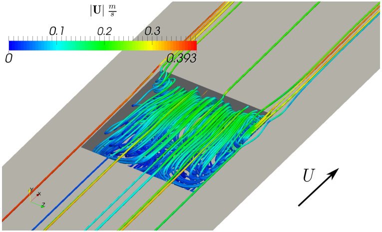

Dimple

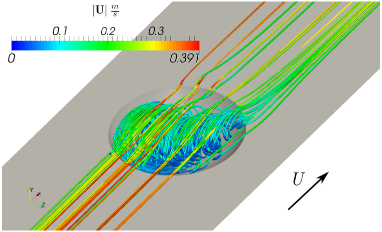

Fouling layer - cavity vs. dimple

- Fouling layer height h_f after 120 s in case of turbulent flow conditions ($\mathrm{Re}_H = 5650$):

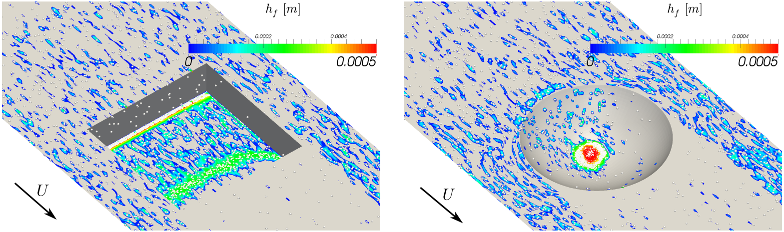

Figure: Fouling layer: cavity (left), dimple (right)

Heat transfer and pressure loss - cavity vs. dimple

- Turbulent cases ($\mathrm{Re}_H = 5650$):
  - I: without particle injection (clean surface)
  - II: $d_p = 100\ \mu$m, particle rate: $500\ 1/\mathrm{s}$
  - III: $d_p = 50\ \mu$m, particle rate: $10000\ 1/\mathrm{s}$

○ channel
● dimple
● cavity

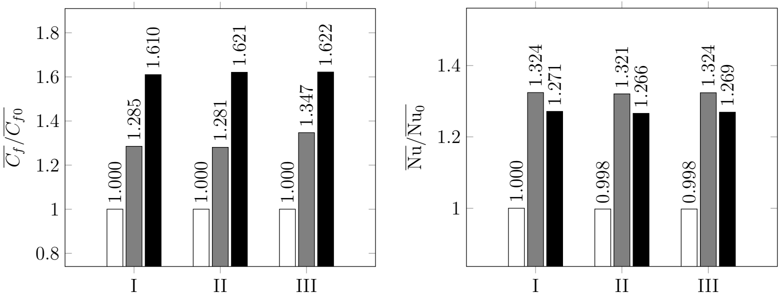

Figure: Comparison of the friction coefficients and Nusselt numbers ($t = 120$ s)

Fouling rate

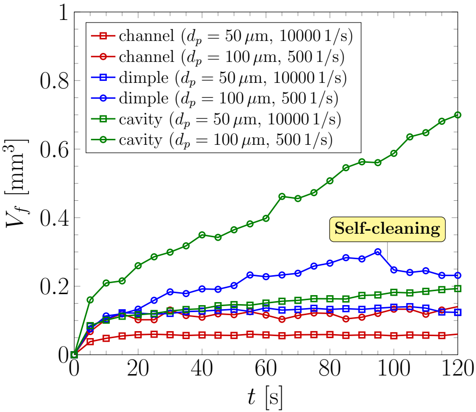

Figure: Total fouling volume for $\mathrm{Re}_H = 5650$

- Less particulate fouling in case of turbulent flows in contrast to laminar flows
- Lowest fouling rates for turbulent dimple flow

  → **possible self-cleaning process due to local turbulent vortex structures** (needs further investigations)

Outline

Introduction

Modeling and implementation
- Euler-Lagrange approach
- Lagrangian particle tracking
- Deposition of particles
- Reaction of the particulate fouling on the carrier fluid
- Heat transfer
- Erosion of the fouling layer

Results
- Validation and verification of the Lagrangian particle tracking
- Particulate fouling on structured heat transfer surfaces

Conclusion and outlook

Conclusion and outlook

- Conclusion:
  - Development / implementation of an universal approach for the simulation of particulate fouling on structured heat transfer surfaces
  - Successfull verification and validation of individual parts of the implementation
- Outlook:
  - Simulation of particulate fouling for more complex structured surfaces
  - Detailed analysis of the interaction between particulate fouling and local vortex structures
  - Further development of the condition for particle deposition and conversion

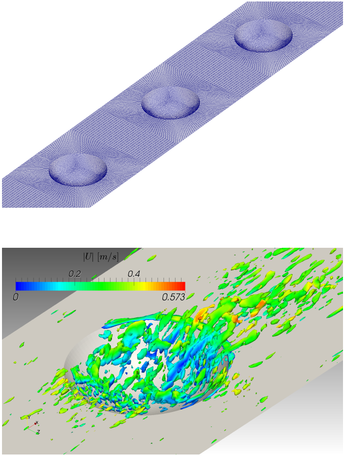

Figure: Dimple row (above), λ_2-vortex structures inside a dimple (below)

Thank you for your attention!

Acknowledgment

- DFG
- HLRN

Dr.-Ing. Johann Turnow

University of Rostock
Faculty of Mechanical Engineering and Marine Technology
Chair of Modeling and Simulation
Albert-Einstein-Str. 2
18059 Rostock
Email: johann.turnow@uni-rostock.de